Low Dose Carotid CT Angiography with Pure Iterative Reconstruction.

Kevin P Murphy[1], Maria Twomey[1,2] , Lee Crush[1], Patrick D McLaughlin[3], Emma M Canniffe[1], Louise Baker[2], Brian M Manning[4], Gerald Wyse[2], Noel Fanning[2], Owen J O'Connor[1,2], Michael M Maher[1,2].

[1]Department of Radiology, University College Cork, Cork, Ireland.

[2]Department of Radiology, Cork University Hospital, Cork, Ireland.

[3]Department of Emergency and Trauma Radiology, Vancouver General Hospital, Vancouver, British Columbia, Canada.

[4]Department of Vascular Surgery, Cork University Hospital, Cork, Ireland.

*Corresponding author:

Professor Michael M Maher.

Email: *M.Maher@ucc.ie*

Tel: 00 353 21 4920274.

Fax: 00 353 21 4920319

Abstract

Purpose:

Materials and Methods:

Results:

Conclusions:

Keywords: Carotid CT, Stroke; CT angiography; low dose CT; iterative reconstruction.

Introduction:

Materials and Methods:

Institutional ethical board approval was granted for this prospective study. The study population consisted of twenty consecutive patients who underwent CT angiography (CTA) of the carotid arteries between February 2012 and September 2012. These were patients with known or suspected carotid artery disease, which were referred for clinically indicated CTA of the carotid arteries. Written consent was obtained from each subject. The inclusion criteria consisted of adults that were referred from the vascular, geriatric or neurology services, that required a carotid CTA as part of their carotid artery disease work-up and management, that were scanned during normal daytime working hours and that were able to consent to be included in the study. All patients outside of these criteria were excluded.

Image Acquisition

All studies were performed on a 64-slice Lightspeed VCT (GE Healthcare, GE Medical Systems, Milwaukee, USA). All participants consented to have two contemporaneously acquired studies. The protocol for the two carotid CTA examinations was designed so that the combined radiation exposure from both scans did not exceed that of a single conventional carotid CTA. This was achieved by dividing the radiation dose of the carotid CTA into two quotients. The first (conventional dose) CT acquisition used a radiation dose of approximately 70%

of the dose of a standard carotid CTA. The second (low dose) CT acquistition used 30% of the dose of a standard carotid CTA. Each subject received 100mls of non-ionic intravenous contrast media contrast media (iohexol, Omnipaque 350, GE Healthcare, Mississauga, ON, Canada) at a rate of 5ml per second followed by a 20ml saline bolus injected via a power injector (Stellant; Medrad, Warrendale, PA). Automatic bolus-tracking software (SmartPrep; GE Healthcare) was used to monitor and identify peak arterial (150 Hounsfield Units, HU) and acquisition commencement. There was a 3-second delay between completion of the conventional dose protocol and the start of the low dose scan.

The conventional dose protocol used the following parameters: tube voltage, 100 kV; gantry rotation time, 0.4 seconds; tolerated noise index, 38%; and automatic tube current modulation threshold range of 60mA -230mA. The following scanning parameters were utilised for the low dose study: tube voltage, 100 kV; gantry rotation time 0.4 seconds; tolerated noise index 70%; and automatic tube current modulation threshold range of 30mA -150mA.

CT image reconstruction

Images were reconstructed from an acquisition thickness of 0.625 mm to a final slice thickness of 2 mm. The conventional dose data was reconstructed using standard department protocol employing hybrid IR, (60%FBP, filtered back projection and 40% ASiR, adaptive statistical iterative reconstruction, labeled CD ASiR, (GE Healthcare, GE Medical Systems, Milwaukee, USA). The low dose data was reconstructed with pure IR (Model Based Iterative Reconstruction (MBIR) Veo (GE Healthcare, GE Medical Systems, Milwaukee, USA)), labeled LD MBIR in addition to 40%ASiR, named LD ASiR.

CT Dose Measurement

Dose length product (DLP) and volume Computed Tomography dose index ($CTDI_{vol}$) values were recorded from each CT dose report. $CTDI_{vol}$ and DLP tolerances were verified using a standard 32cm perspex phantom, a 10cm ionization chamber with a Victoreen NERO mAx unit (Fluke Biomedical, OH, USA). The 32cm phantom was imaged at tube currents of 40mA and 50mA with a 32cm FoV. Radiation measurements were taken with the pencil chamber inserted at central and peripheral locations. Three measurements at each location were averaged and used to calculate corresponding CTDI values which were subsequently converted to a weighted CTDI. The displayed CTDI and DLP values of the CT console were recorded and percentage error calculated using ionization chamber measures. Calibration of the CT unit was performed once per week in accordance with the manufacturer's instructions.

The Imaging performance and assessment in CT patient dosimetry calculator (ImPACT version 0.99x, London, England) was used to calculate effective dose (ED). The radiation exposure resultant from the CT topograms was excluded from analysis.

Objective Image Quality Analysis

Objective image quality measurements were performed by 1 radiologist (KM, 5 years experience) on a dedicated workstation (Advantage Workstation VolumeShare 2, Version 4.4, GE Medical Systems, Milwaukee, WI). 3mm spherical regions of interest (ROI) (10.6mm^3 volume) were placed in 49 individual anatomical regions on each dataset. Intravascular measurements

were taken bilaterally at the following levels: common carotid origin (CCA), CCA bifurcation, superior extracranial internal carotid artery (ICA), terminal intracranial ICA, vertebral artery origin (V1), mid V2 vertebral artery segment and V4 vertebral artery division. Measurements were recorded bilaterally by placing the ROI in the adjacent sternocleidomastoid muscles at the 7 vascular levels. If the sternocleidomastoid was not on the image at the relevant level, the pectoralis major or temporalis muscles were utilised. Background noise was recorded by placing the ROI 5mm from the skin on 3 occasions at each of the 7 levels. ROIs were placed in as homogenous an area as possible. The mean attenuation in Hounsfield units (HU) and standard deviation of the mean attenuation was recorded for each ROI. The standard deviation of the mean attenuation was used as the objective measure of noise (1–3). These measurements were used to calculate the contrast to noise and signal to noise ratios using previously validated methods (4). Contrast to noise ratio (CNR) was calculated for each of the 7 arterial segments bilaterally using the following equation: CNR = (mean intravascular HU – mean HU of adjacent sternocleidomastoid muscle) / mean background ROI standard deviation (4). Signal to noise ratio (SNR) was calculated at the same levels using the following: SNR = mean intravascular HU / mean background ROI standard deviation (4).

Subjective Image Analysis

Subjective image quality parameters and grading system were adapted from the European Guidelines on Quality Criteria for CT document (5) and were selected on the basis of findings of previous studies (6,7). Subjective quality assessment was performed in consensus by 2 readers (MMM, 18 years experience; OJOC, 9

years experience). One of the observers (MMM) was familiar with these methods of assessment, having successfully used them previously (3,8,9) and trained the other reader (OJOC) prior to analysis using a training set of five standard CTs. Subjective image noise, contrast resolution and spatial resolution were scored using a ten-point scale at 7 anatomical levels: right common CCA, right CCA bifurcation, superior extracranial ICA, terminal ICA, right vertebral artery origin (V1), mid V2 vertebral artery segment and V4 vertebral artery division. Subjective image noise was graded according to the extent of "graininess" or "mottle" present on CT images and was graded as acceptable (score of 5) if average graininess was seen with satisfactory depiction of small anatomic structures such as the blood vessels and interface between structures of variable attenuation, unacceptable (score of 1) if graininess interfered with depiction of these structures, and excellent (score of 10) where there was minimal or no appreciable mottle. Contrast resolution and spatial resolution were scored at the same 7 anatomical levels. With regard to contrast resolution, a score of 10 represented superior contrast depiction between different soft tissues, a score of 1 indicated the poorest contrast and 5 indicated acceptable contrast. In terms of spatial resolution, a score of 10 represented excellent edge detail, a score of 1 indicated poor spatial resolution and a score of 5 designated acceptable spatial resolution. The presence and impact of streak artefact was scored at each of the 7 anatomical levels using a 3-point scheme: (0 - no streak artefact; 1 - streak artefact present but not interfering with image interpretation; 2 - streak artefact present and interfering with image interpretation). Diagnostic acceptability was graded as acceptable (score of 5), unacceptable (score of 1) or excellent (score of 10) respectively, if depiction of soft-tissue structures for diagnostic

interpretation and degree of image degradation by beam-hardening artifacts was satisfactory, unsatisfactory, or considerably superior. This was assessed for the aortic arch, carotid system, vertebrobasilar system, venous sytem, thyroid gland and non-thyroid soft tissues individually.

Diagnostic performance

The degree of ICA stenosis was calculated with the use of a semi-automated vessel analysis tool on a dedicated workstation (Advantage Workstation VolumeShare 2, Version 4.4) in a blinded fashion by 2 radiologists in consensus (LC, 6 years experience; MOK, 3 years experience). This was performed as per NASCET (North American Symptomatic Carotid Endarterectomy Trial) criteria (10–12), whereby the minimum diameter of the proximal ICA stenosis was compared to the diameter of the parallel-walled superior cervical ICA. The automated calculation tool was utilised but manual methods were substituted if the readers deemed the tracking to be inaccurate. The stenoses were graded into insignificant (<50%), moderate (50-69%), severe (70-90%) and critical (>90%). The gradings were compared for each reconstruction. Using the CD ASiR images as the 'gold standard', the mean deviation for the absolute ICA stenosis value for each patient was compared for LD ASiR and LD MBIR reconstructions.

Statistical Analysis

All statistical tests were performed with a commercially available medical statistical package Statistical Package for Social Scientists (SPSS) version 20.0 (IBM, Armonk, NY). Wilcoxon signed rank test was used for statistical analysis to compare non-parametric qualitative parameters. Normally distributed

parametric quantitative indices were compared using a paired t-test. Agreement between stenosis grading was compared using Cohen's κ test of agreement. Deviation from the 'gold standard' ICA stenosis value was calculated via a mean-difference / Bland Altman calculation. A difference with a *p* value of <0.05 was considered statistically significant. All data are presented as mean ± standard deviation or median ± interquartile range unless otherwise stated.

Results:

20 patients participated (60% male, 65% smokers, 85% diabetics, 66.74±6.74 years).

Radiation Exposure

Mean dose length product (DLP) and effective dose (ED) for the low dose studies were 341.33mGy.cm (range 278.88-411.36mGy.cm) and 1.84mSv (range 1.51-2.22mSv) respectively. Mean dose indices for the conventional dose studies were 687.96mGy.cm (DLP range 563.51-1169.24mGy.cm) and 3.71mSv (ED range 3.04-6.31mSv). The low dose studies were significantly lower (p<0.001), with a mean reduction of 49.6%.

Objective Image Quality Evaluation

Image CNR and SNR parameters are denoted in figures 1 & 2 in addition to table 1. CNR and SNR measurements on the low dose ASiR images were significantly inferior to both the LD MBIR and CD ASiR images at all levels (p<0.01 for all comparisons). There was no significant difference in terms of SNR or CNR between LD MBIR and CD ASiR assessments at most levels. LD MBIR SNR and

CNR were significantly superior ($p<0.05$) to LD ASiR at the CCA origin and LD MBIR CNR was significantly superior at V1 ($p=0.004$). Summating all measurements, LD MBIR were insignificantly superior when compared to CD ASiR images in terms of CNR (82.93±80.74 Vs. 77.67±43.91)($p=0.284$) and SNR (99.06±88.97 Vs. 89.78±46.79)($p=0.085$).

Subjective Image Quality Analysis

Results from subjective image quality assessment are shown in figure 3. CD ASiR images were significantly superior in terms of subjective noise when compared with LD ASiR (median ± IQR, 7.5±1 vs. 7±2, $p<0.001$) and LD MBIR (7.5±1 vs. 7±1, $p<0.001$). LD MBIR subjective image noise was significantly superior to LD ASiR image assessment in addition ($p=0.036$). In terms of spatial resolution, LD MBIR was deemed superior to CD ASiR (8±0 vs. 7±1, $p=004$) and LD ASiR images (8±0 vs. 7±1, $p<0.001$). LD MBIR contrast resolution was also superior to CD ASiR (8±1 vs. 7±1, $p=0.002$) and LD ASiR images (8±1 vs. 7±1, $p<0.001$). LD MBIR was superior to the other datasets with regard to diagnostic acceptability (LD MBIR: 9±1, CD ASiR: 8±1, LD ASiR: 7±1; $p<0.001$ for all comparisons). In addition, CD ASiR was superior to LD ASiR with regard to same ($p<0.001$). Non-vascular soft tissue diagnostic acceptability was also superior for LD MBIR (8±0) when compared to CD ASiR (7±0, $p<0.001$) and LD ASiR (6±1, $p<0.001$). Streak artefact reduction was also superior on the LD MBIR reconstructions (1±1) when compared to the CD ASiR (2±0, $p<0.001$) and LD ASiR (1±0, $p<0.001$) reconstructions.

Diagnostic Performance

Of the 40 (20 patients) internal carotid arteries assessed, 6 were occluded. All of these were correctly identified on both low dose reconstructions. Of the remaining 34 patent ICAs, 24 had stenoses of <50%, 3 had moderate stenoses of 50-69%, 5 had severe stenoses of 70-90% and 2 had critical stenoses >90%. For the non-occluded ICAs, there was excellent agreement for stenosis grading accuracy when the LD ASiR (Cohen's $\kappa = 0.806$) and LD MBIR (Cohen's $\kappa = 0.806$) were compared to the CD ASiR assessment. Both the LD MBIR and LD ASiR underestimated a single stenosis grading from '50-69%' to '<50%' in 2 different patients. With regard to Bland-Altman / mean-difference performance of the low dose reconstructions, both the LD MBIR and LD ASiR studies underestimated the stenosis (LD MBIR: -3.23±5.81%; LD ASiR: -3.65±8.46%) when the absolute per cent stenoses values were compared with the CD ASiR images. LD MBIR was insignificantly superior ($p=0.811$). When the calculated diameters of the superior cervical ICA were examined, there was no significant difference between mean LD ASiR (5.43±0.94mm) and CD ASiR (5.22±0.78mm) calculations ($p=0.130$). Mean diameters calculated on the LD MBIR images (4.89±0.94mm) were less than CD ASiR ($p<0.007$) and LD ASiR ($p<0.001$) measurements.

Discussion:

References:

1. Marin D, Nelson RC, Schindera ST, Richard S, Youngblood RS, Yoshizumi TT, et al. Low-tube-voltage, high-tube-current multidetector abdominal CT: improved image quality and decreased radiation dose with adaptive statistical iterative reconstruction algorithm--initial clinical experience. Radiology. 2010 Jan;254(1):145–53.

2. Craig O, O'Neill S, O'Neill F, McLaughlin P, McGarrigle A, McWilliams S, et al. Diagnostic accuracy of computed tomography using lower doses of radiation for patients with Crohn's disease. Clin Gastroenterol Hepatol. 2012 Aug;10(8):886–92.

3. O'Neill SB, Mc Laughlin PD, Crush L, O'Connor OJ, Mc Williams SR, Craig O, et al. A prospective feasibility study of sub-millisievert abdominopelvic CT using iterative reconstruction in Crohn's disease. Eur Radiol. 2013 Sep;23(9):2503–12.

4. Beitzke D, Wolf F, Edelhauser G, Plank C, Schernthaner R, Weber M, et al. Computed tomography angiography of the carotid arteries at low kV settings: a prospective randomised trial assessing radiation dose and diagnostic confidence. Eur Radiol. 2011 Nov;21(11):2434–44.

5. Bongartz G, Geleijns J, Golding S, Jurik A, Leonardi M, van Meerten E. European guidelines on quality criteria for computed tomography. European Commission. 1999.

6. Siddiki HA, Fidler JL, Fletcher JG, Burton SS, Huprich JE, Hough DM, et al. Prospective comparison of state-of-the-art MR enterography and CT enterography in small-bowel Crohn's disease. AJR Am J Roentgenol. 2009 Jul;193(1):113–21.

7. Winklehner A, Karlo C, Puippe G, Schmidt B, Flohr T, Goetti R, et al. Raw data-based iterative reconstruction in body CTA: evaluation of radiation dose saving potential. Eur Radiol. 2011 Dec;21(12):2521–6.

8. Prakash P, Kalra MK, Kambadakone AK, Pien H, Hsieh J, Blake MA, et al. Reducing abdominal CT radiation dose with adaptive statistical iterative reconstruction technique. Invest Radiol. 2010 Apr;45(4):202–10.

9. Singh S, Kalra MK, Hsieh J, Licato PE, Do S, Pien HH, et al. Abdominal CT: comparison of adaptive statistical iterative and filtered back projection reconstruction techniques. Radiology. 2010 Nov;257(2):373–83.

10. Moneta GL, Edwards JM, Chitwood RW, Taylor LM, Lee RW, Cummings CA, et al. Correlation of North American Symptomatic Carotid Endarterectomy Trial (NASCET) angiographic definition of 70% to 99% internal carotid

artery stenosis with duplex scanning. J Vasc Surg. 1993 Jan;17(1):152–7; discussion 157–9.

11. Fisher M, Martin A, Cosgrove M, Norris JW. The NASCET-ACAS plaque project. North American Symptomatic Carotid Endarterectomy Trial. Asymptomatic Carotid Atherosclerosis Study. Stroke. 1993 Dec;24(12 Suppl):I24–5; discussion I31–2.

12. Gasecki AP, Hachinski VC, Mendel T, Barnett HT. Endarterectomy for symptomatic carotid stenosis. Review of the European and North American Symptomatic Carotid Surgery Trials. Nebr Med J. 1992 Jun;77(6):121–3.

Figures, Tables and Legends:

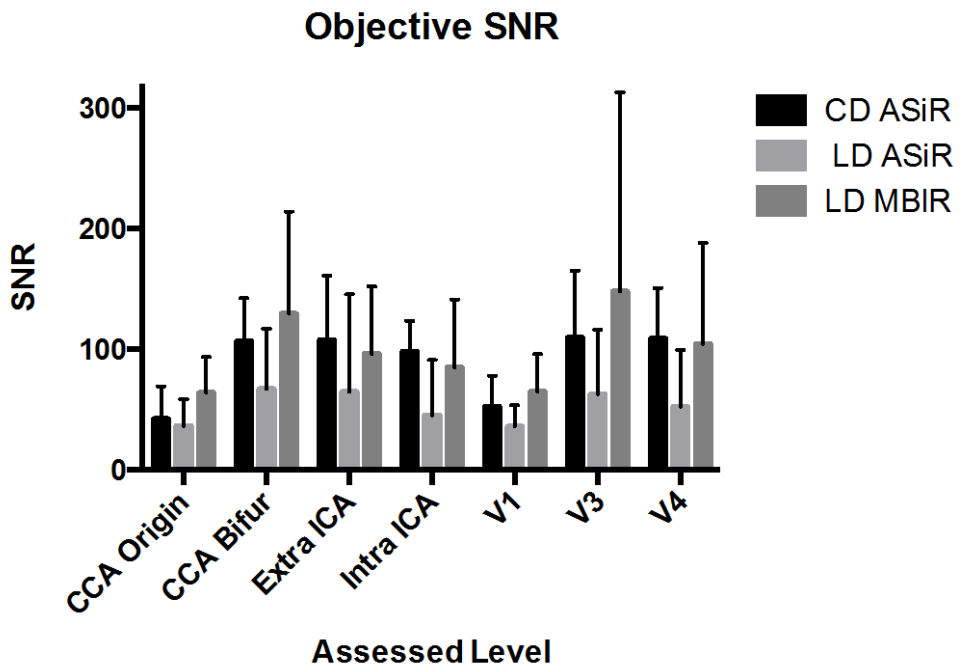

Figure 1. Objective signal to noise ratio (SNR) at the 7 assessed levels (CCA origin, CCA bifurcation, extracranial superior cervical ICA, intracranial terminal ICA, V1 vertebral artery segment, mid V3 vertebral artery segment, V4 vertebral artery division).

Level	Parameter	CD ASiR	LD ASiR	LD MBIR
CCA Origin	SNR	47.28±27.15	36.56±22.11	64.07±29.78*
	CNR	41.24±26.62	31.90±21.29	58.07±29.92*
CCA Bifurcation	SNR	106.92±35.72	67.30±49.94	129.76±84.40
	CNR	94.45±32.30	58.05±45.72	110.04±74.26
Extracranial ICA	SNR	107.81±53.50	64.99±80.77	96.47±55.55
	CNR	95.28±50.04	53.80±70.49	79.52±48.30
Intracranial ICA	SNR	98.27±25.42	45.46±45.77	85.14±56.35
	CNR	87.08±26.17	38.12±40.46	64.87±45.93
V1	SNR	52.55±25.65	36.04±17.80	64.82±31.40
	CNR	37.95±25.44	27.78±18.34	53.98±30.31*
V3	SNR	109.96±55.11	62.67±53.78	148.05±165.14
	CNR	95.56±49.50	52.62±49.44	126.99±154.62
V4	SNR	109.22±41.48	52.66±46.97	104.78±83.69
	CNR	95.66±38.49	44.28±41.68	86.33±74.56
All levels	SNR	89.78±46.79	51.95±49.39	99.06±88.97*
	CNR	77.67±43.91	43.56±44.28	82.93±80.74

Table 1. Objective signal to noise ratio (SNR) and contrast to noise ratio (CNR) at the 7 assessed levels (CCA origin, CCA bifurcation, extracranial superior cervical ICA, intracranial terminal ICA, V1 vertebral artery segment, mid V3 vertebral artery segment, V4 vertebral artery division). LD ASiR measurements were significantly inferior ($p<0.01$) for all levels when compared with LD MBIR

and CD ASiR images. Significant differences between LD MBIR and CD ASiR images are denoted by *.

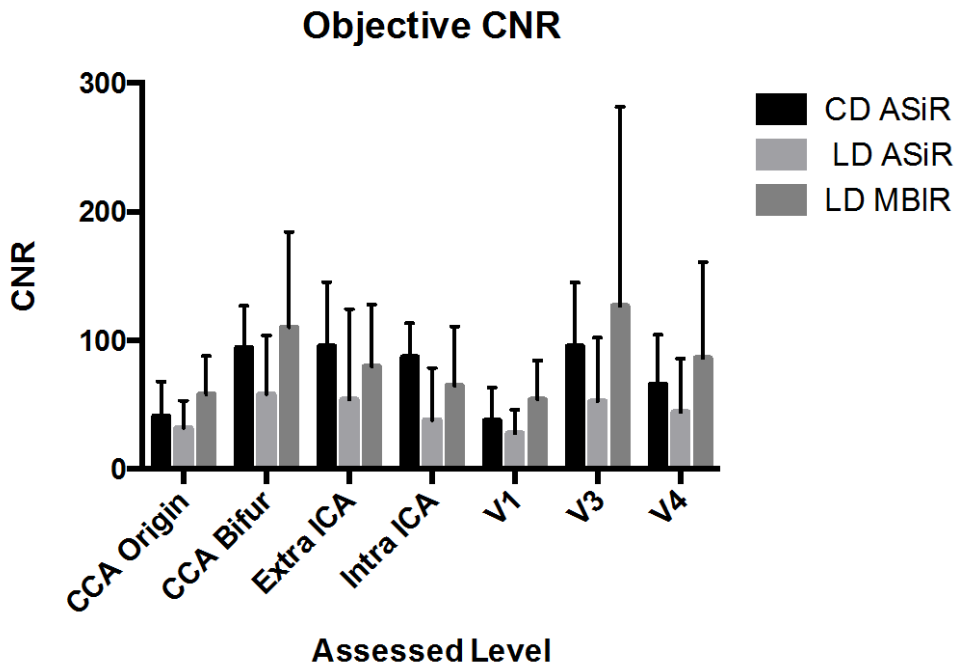

Figure 2. Objective signal to noise ratio (SNR) at the 7 assessed levels (CCA origin, CCA bifurcation, extracranial superior cervical ICA, intracranial terminal ICA, V1 vertebral artery segment, mid V3 vertebral artery segment, V4 vertebral artery division).

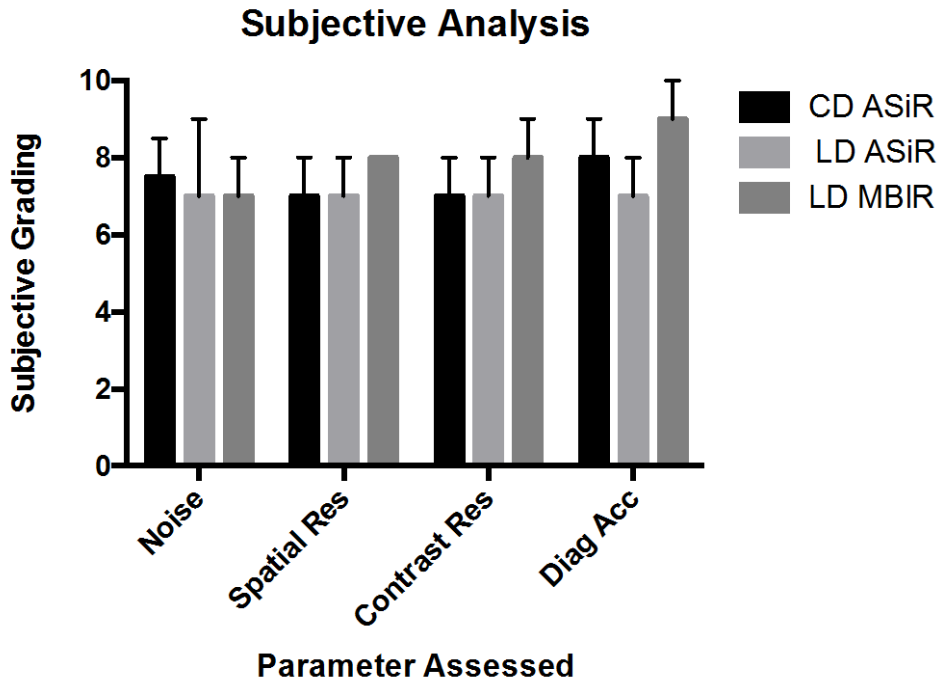

Figure 3. Subjective analysis of image noise, spatial resolution, contrast resolution and diagnostic acceptability (diag acc).